diversity

MDPI

Article

Phylogeographic and Morphological Analysis of *Botrylloides niger* Herdman, 1886 from the Northeastern Mediterranean Sea

Berivan Temiz [1,2], Esra Öztürk [2], Simon Blanchoud [3,*] and Arzu Karahan [2,*]

[1] Developmental Biology and Genomics Laboratory, Department of Anatomy, Otago School of Medical Sciences, University of Otago, P.O. Box 56, Dunedin 9054, New Zealand
[2] Institute of Marine Sciences, Middle East Technical University, Erdemli-Mersin 33731, Türkiye
[3] Department of Biology, University of Fribourg, 1700 Fribourg, Switzerland
* Correspondence: simon.blanchoud@unifr.ch (S.B.); arzukarahan@ims.metu.edu.tr (A.K.)

Abstract: *Botrylloides niger* (class Ascidiacea) is an invasive marine filter-feeding invertebrate that is believed to originate from the West Atlantic region. This species of colonial tunicate has been observed in several locations along the coasts of Israel and around the Suez Canal, but it has not yet been reported on the coasts of the Northeastern Mediterranean Sea (NEMS), suggesting an ongoing Lessepsian migration. However, the extent of this invasion might be concealed by reports of other potentially misidentified species of *Botrylloides*, given that the strong morphological similarities within this genus renders taxonomical identification particularly challenging. In this study, we performed a phylogeographic and morphological analysis of *B. niger* in the NEMS. We collected 238 samples from 8 sampling stations covering 824 km of the coastlines of NEMS. We reported 14 different morphotypes, of which the orange-brown, orange, and brown-striped morphs were the most abundant. Using the mitochondrial cytochrome C oxidase I (COI) as a DNA barcode marker, we identified 4 haplotypes. The COI haplotypes clustered with the reference *B. niger* sequences from GenBank and differed significantly from the sister *Botrylloides* species. We confirmed our identification using three additional barcoding markers (Histone 3, 18S rRNA, and 28S rRNA), which all matched with over 99% similarity to reference sequences. In addition, we monitored a station for a year and conducted a temporal analysis of the collected colonies. The colonies were absent during the winter and spring, while new colonies were established in the summer and expanded during autumn. We performed demographic population analysis on our spatial data that identified a possible population subdivision at a sampling site, which might have been caused by local freshwater input. Herein, we present the first report on the presence of *Botrylloides niger* in the NEMS. This study represents a key step toward understanding the diversity and the propagation of this highly invasive species of colonial ascidians, both within the Mediterranean basin as well as globally.

Keywords: ascidian; DNA barcoding; COI; northeastern Mediterranean Sea; phylogeography

Citation: Temiz, B.; Öztürk, E.; Blanchoud, S.; Karahan, A. Phylogeographic and Morphological Analysis of *Botrylloides niger* Herdman, 1886 from the Northeastern Mediterranean Sea. *Diversity* **2023**, *15*, 367. https://doi.org/10.3390/d15030367

Academic Editor: Stephan Koblmüller

Received: 4 December 2022
Revised: 28 February 2023
Accepted: 1 March 2023
Published: 3 March 2023

1. Introduction

Phylogeography investigates the geographical distribution of genealogical lineages by combining spatial snapshots of a portion of a population [1]. Populations divided by long distances or geographical barriers may display a higher level of genetic differentiation, representing the accumulation of mutations acquired over long periods of isolation [2]. Geography is, thus, intrinsically connected with evolutionary relations, and this connection can be detected via molecular markers that estimate genetic variations to understand the linkage between populations [1]. Consequently, spatial analyses of genetic diversity can provide important insights into the evolution of entire populations over potentially large spatial and temporal scales.

While such analyses are reasonably accessible in terrestrial environments, in aquatic systems, the population dynamics are more turbulent and harder to estimate. Considering

the development of maritime traffic and aquaculture, the establishment of non-indigenous marine organisms in new environments is inevitable [3]. In particular, the global spreading of invasive species is a major threat to native ecosystems, and their prevention is of major biological and economical interest. Thus, phylogeographic studies on marine environments are essential to estimate genetic diversity, isolation patterns, and hydrographic barriers to elucidate the dispersal of populations.

DNA barcoding is a prominent molecular tool used to identify species and catalogue biodiversity. The main marker used for barcoding is a 500–650 bp fragment of the mitochondrial cytochrome C oxidase subunit I (COI) gene. COI sequences are compared to global reference databases, such as GenBank or Barcoding of Life Database (BOLD) [4,5], to assign to the sample of interest the same species as the one of the closest sequences found among the references. COI sequences from the same population can be compared to estimate the genetic diversity of the population and identify haplotypes [6]. COI sequences can also be compared across spatial and temporal sampling locations to study the movement of genetic material and infer population dynamics [7]. Additional genetic markers include the sequences of the chromatin component Histone 3 (H3), the ribosomal small subunit 18S rRNA, and the ribosomal large subunit 28S rRNA, all of which have been used to resolve population dynamics [8].

In the Northeastern Mediterranean Sea (NEMS), encompassing the coasts of Türkiye, Syria, and Lebanon, DNA barcoding studies have increased in recent years to monitor possible invasive Lessepsian migrations from the Suez Canal into NEMS [9]. These studies have proven to be decisive for the implementation of marine conservation policies by providing the required scientific knowledge on the ecosystem's dynamics [9–21].

Botrylloides is a globally present genus of sessile marine invertebrate filter-feeders that belong to the Tunicata subphylum [22]. These colonial chordates live on hard substrata by establishing flat, hard, gelatin-encrusted colonies after the motile larva attaches and undergoes metamorphosis [23]. *Botrylloides* can also undergo asexual reproduction, which is called blastogenesis, whereby new zooids bud from the peribranchial wall of the parental zooids [24]. The blastogenic cycle culminates with the death and absorption of all parental zooids by the colony and the emergence of a new generation of zooids in a process known as the takeover [25]. Natural chimerism following the fusion of two closely related kins, hibernation, and even whole-body regeneration have commonly, but not exhaustively, been reported in *Botrylloides* [6,26–31]. The *Botrylloides* genus is composed of 21 reported species, all of which are morphologically similar, with zooids aligned in a ladder-like arrangement. Anatomical features that differentiate species can be extremely difficult to assess, such as the number of stigmata rows on the branchial basket, the presence of a pyloric caecum, or the location where the larvae incubate. Consequently, taxonomical assignments based on their anatomical features are challenging for species-level categorization [32].

Several species of *Botrylloides* have been identified as invasive and have been reported in the Mediterranean Sea [10,32–41]. *Botrylloides niger* [42] is classified within the Styelidae family and has been synonymized with reports of other colonial ascidians, including *Metrocarpa nigrum* [42], *Botryllus niger* [42], *Botryllus nigrum* [42], *Botrylloides chazaliei* [43], and *Botrylloides nigrum* [42]. *B. niger* is predicted to be native to the West Atlantic due to its frequent presence there, although it was first identified on the coasts of Bermuda, an island located in the temperate region of the North-Atlantic Ocean [6]. Peres documented the presence of *B. niger* on the Mediterranean coasts of Israel more than fifty years ago [44], a presence that was recently confirmed using DNA barcoding by Griggio et al. [45,46]. Since then, Halim and Messeih have reported its presence in the Suez Canal [41]; Sallona et al. in the Ionian Sea [47]; and Crocetta et al. at several sites in Italy [48–50].

The only record of *Botrylloides* in the NEMS is that of *Botrylloides leachii*, documented in the Mersin harbor in Türkiye [36]. However, this report was solely based on morphology and has a number of missing key anatomical insights, which suggests that the resulting taxonomical assignment at the species level could be debatable. In particular, pigmentation patterns of colonial ascidians were shown to be highly polymorphic, and, thus, not suitable

for species determination [51]. For instance, Brunetti [38] and Reem et al. [10] disagree with Sheets et al. [6] on the identification of *Botrylloides* colonies on the coasts of Israel, with the former two assigning them as *B. leachii,* but the latter as *B. niger*.

In this study, we investigated the genetic and morphological diversity of *B. niger* colonies from the NEMS by combining COI barcoding with H3, 18S rRNA, and 28S rRNA to support our identification, and conducted a time-series sampling for a year to investigate the effect of seasonal changes on population genetics. Herein, we present the first report on the presence of *Botrylloides niger* in the NEMS. This study is a key step towards understanding the diversity and the propagation of this highly invasive species of colonial ascidians, both within the Mediterranean basin and globally.

2. Materials and Methods

2.1. Colonies Sampling

Spatial samples were collected from the coastal areas of the Antalya (Kemer-Side-Alanya-Tersane), Mersin (Tisan-Kızkalesi-Mezitli), and Hatay (Konacık) sites in September and October 2018 at water depths between 30–50 cm, as previously described for *Botrylloides anceps* (Figure 1A) [31]. Samples were collected from submerged stones using a single-edged razor blade. The colonies to be monitored were placed onto a microscope slide and attached with a sewing thread, while the samples for barcoding were put into 1.5 mL tubes filled with 70 % (*v*/*v*) ethanol. The sampling area's date, coordinates, salinity, and pH were documented (Table S1). In total, 238 samples were collected, 203 of them to be processed for DNA barcoding (Table S2). Of these samples, 100 were used in our spatial analysis, 65 in the temporal analysis, and 38 in both analyses. The Kızkalesi station was visited monthly for the time-series between November 2017 and October 2018, with samples collected in November 2017 and between July 2018 and October 2018 (Table S3).

2.2. Colonies Characterization

A total of 218 of our specimens were characterized via morphological examination regarding their zooid distribution, color, and habitat preferences. Pigmentation patterns for each morphotype (Figure S1) were characterized by adapting the criteria used for the sister genus *Botryllus* [51]. Living specimens that were taken to the laboratory were photographed under a stereo and a light microscope (Olympus SZX16-UC30 camera; Olympus CX43-ToupTek camera (Olympus, Tokyo, Japan; ToupTek Photonics, Hangzhou, China). Living colonies were kept at 20 °C in the IMS-METU aquaculture room. The temperature and light of the room were stable, and the salinity of the water was constant at 40 ppt. The colonies were fed and the water was replaced every two days.

Hibernation of the animals was characterized by visual inspection based on the regression of all the zooids, thus resulting in a dense vascular system. Blastogenic cycles were monitored from the ventral side of the zooids, and the budding through the atrial epithelium was monitored by visual inspection.

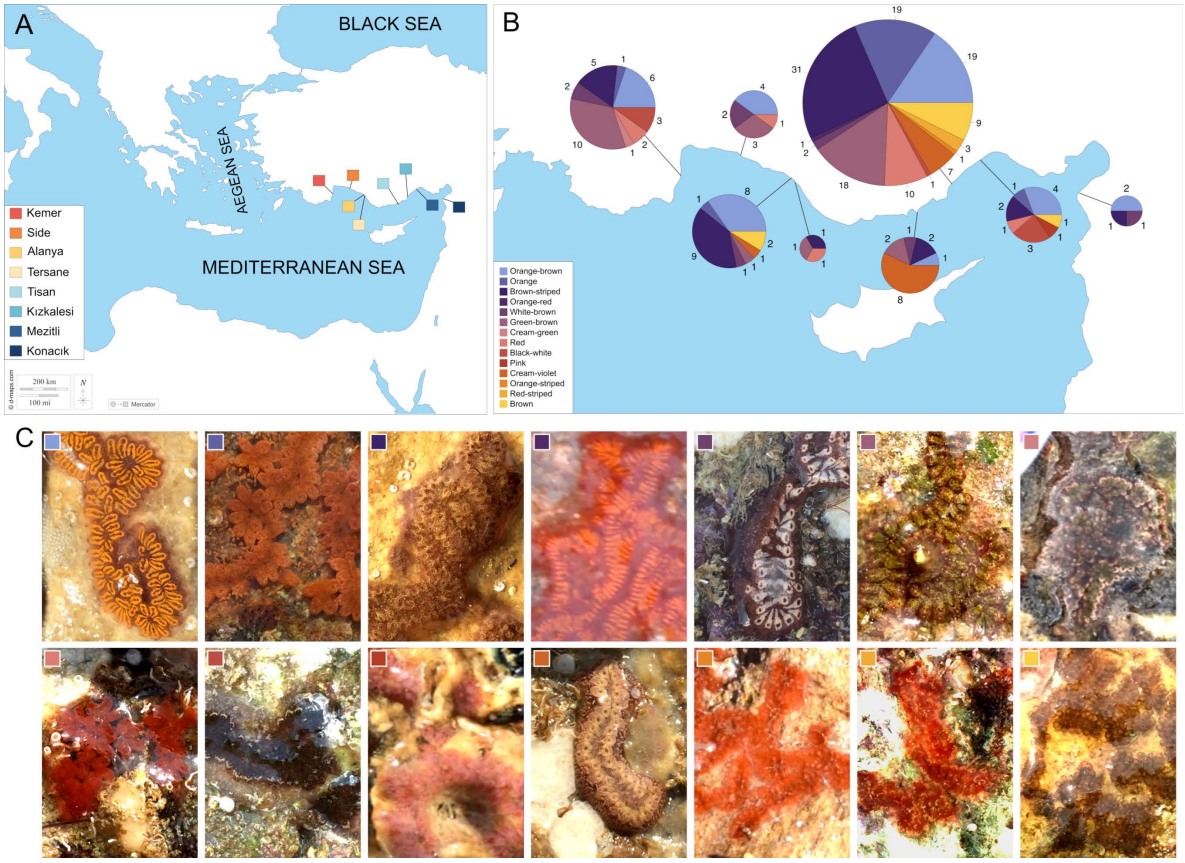

Figure 1. Morphotypes of *Botrylloides niger* from the sampling stations of the NEMS. (**A**) NEMS sampling sites, from west to east, cover the Antalya region (Kemer, Side, Alanya, Tersane), the Mersin region (Tisan, Kızkalesi, Mezitli) and the Hatay region (Konacık). (**B**) Regional diversity in the sampled morphotypes, depicted with pie charts proportional to the sample sizes. (**C**) In situ images of the corresponding morphotypes.

2.3. Molecular Analyses

DNA extractions were completed as previously described [31]. The amplification reactions were executed as previously described [10] for the COI, H3, 18S, and 28S genes (Table S4). All PCR products were purified with the NucleoSpin® DNA clean-up kit [52] and then sent to Macrogen Inc. (Seoul, Republic of Korea) for sequencing. The primers used in this study are given in Table S5. Sequences were aligned for each gene region separately using Clustal X v2 [53]. Acquired contigs were aligned on BioEdit version 7 [54], edited, and trimmed.

2.4. Haplotypes Network Analyses and Bayesian Trees

The minimum spanning network of haplotypes were calculated using Arlequin version 3.5.2.2 [55] and visualized via HapStar version 0.7 [56].

Bayesian trees of COI haplotypes and database-mined samples show the phylogenetic distances. The best model for the MrBayes v3.2 [57] was chosen via PhyML-SMS v3 software [58]. In total, four MrBayes runs (two independent for each) were conducted for the haplotypes (H) alone, as well as together, with all the database-mined samples (DM). The runs were performed based on the general time-reversible model with a proportion of invariable sites (GTR + I) for 900′000 (H) and 5′400′000 (DM) combined states with two independent runs. In total, 15 (H) and 45,002 (DM) trees were sampled after discharging a burn-in fraction of 25 % that verified the log likelihood of the cold chain (LnL) stationarity. As the convergence diagnostic, the average standard deviation of split frequencies was recorded as 0.004 (H) and 0.005 (DM), and potential scale reduction factors (PSRFs) were close to 1.0 for both [57]. The sister group of *Botrylloides*, the colonial ascidian *Symplegma*,

was used as an out-group. The validity of the MCMC chains was confirmed by visual inspection of the LnL distribution to ensure stationarity. The final trees were visualized with FigTree v.1.4.4 [59].

2.5. Database Sequences

Ascidian sequences were mined from NCBI GenBank [4] in September 2022 to be used for species delimitation analyses. Sequences were selected based on their assigned genera, whether they had a voucher record, and whether they were approved by a taxonomist. All utilized reference sequences are listed in Table S6.

2.6. Species Analyses

Species delimitation analyses were carried out using the Automatic Barcode Gap Discovery method through the Assemble Species by Automatic Partitioning (ASAP, https://bioinfo.mnhn.fr/abi/public/asap/asapweb.html, accessed on 20 September 2022) [60] and the Poisson Tree Processes (PTP, http://species.h-its.org/ptp/, accessed on 20 September 2022) [61]. The hypothetical species are defined as Operational Taxonomic Units (OTUs) using these methods. ASAP clusters sequences into partitions consisting of hypothetical species based on the statistical inference of the "barcode gap", i.e., the gap in the distribution of intra-species and inter-species pairwise distances. ASAP analyses were performed using a web-based interface [60] (last accessed on 20 September 2022). Two metric options provided by ASAP for the pairwise distance calculations were used: Jukes–Cantor (JC69) [62] and Kimura 2 parameters (K80) [63]. This strategy allowed us to exclude possible biases of the selected evolutionary model for OTU delimitation. PTP analyses were conducted using the Bayesian implementation (bPTP; adds Bayesian support values to delimited species on the input tree), available on the web-based interface [61] (last accessed on 20 September 2022). MrBayes trees were generated using 100′000 Markov Chain Monte Carlo (MCMC) generations, subsampling every 100 generations, a burn-in fraction of 0.1, and 123 seed.

2.7. Population Analyses

Mean COI distances between the NEMS populations and the NCBI database sequences were calculated by a Kimura 2-parameter model [64] using MEGA version X [65]. The Blast suite of NCBI was used to find the matching substitution rates between bases [66]. The population-wide statistics, including the genetic diversity, neutrality test, and genetic differentiation, were calculated from the corresponding multiple sequence alignments of the COI locus per population with DnaSP version 6 [67].

The following four genetic diversity indices were measured: number of polymorphic sites (N_p), number of haplotypes (N_h), nucleotide diversity (π; window length: 100, step size: 25) [68], haplotype diversity (H_d, window length: 100, step size: 25) [69]. In addition, three associated neutrality test statistics were computed to test the hypothesis that all mutations were selectively neutral: Fu and Li's D* (F&LD) [68], Fu and Li's F* (F&LF) [70], and Tajima's D (TajD) [71].

To compare populations, the pairwise genetic differentiation (F_{st}, permutations number: 10,000) [72,73] and the population size changes were calculated with DnaSP. For the population size change, measured population mismatch distributions were compared to expected values for a population with a constant population size [74] using the raggedness statistic, *r* [75].

All figures were edited with Inkscape version 1.1 [76].

3. Results

3.1. Morphological Records

Overall, 14 different morphotypes were observed among the sampled colonies (Figure 1). Single- and double-colored morphs were recorded: orange-brown, orange, brown-striped, orange-red, white-brown, green-brown, cream-green, red, black-white, pink, cream-violet,

orange-striped, red-striped, and brown (Figure S1). These 14 major morphotypes were composed of multiple sub-types with minute differences in the patterns of the colors.

All colonies presented the typical *Botrylloides* ladder-like organization, where zooids are aligned side by side while their dorsal lamina face the surrounding environment, and the ventral side is located on the attachment side (Figure S2). Four large and four small tentacles were recorded inside the buccal siphon, and eight alternative smaller protrusions were observed (Figure S2). Pigmented blood cells were recorded on the tentacles, especially on the two largest ones. Many pigmented blood cells on both sides of the endostyle were observed over the whole length of the animals.

3.2. Life History

The blastogenic cycle of 19 colonies was examined according to the Watanabe [77] four-phase (A–D) staging method. The duration of the cycle varied between 4 to 7 days (Figure S3). In stage A, two primary blastozooids were formed by budding from a single parental zooid. During stage B, blood flow was observed in the cardiac swellings of the primary buds. In stage C, secondary blastozooids were formed from the primary zooids. In stage D, known as takeover, the parental zooids were reabsorbed by the colony while the clonal primary zooids matured (Figure S3).

Fourteen of the nineteen cultured colonies hibernated during the winter season. During hibernation, there were no zooids in the dormant colony. The overall morphology thus consisted of only a carpet-like layer of ampullae (Figure S4). The blood circulation was lower and thicker than what is usually observed in healthy colonies. Termination of hibernation was not observed in any colony, even after the end of winter.

The life spans and morphologies of 19 colonies were documented (Table S7). The average life span of the *B. niger* colonies under lab conditions was ~5 months.

3.3. Network Analysis Based on COI

Our samples clustered under four haplotypes; H1, H2, H3, and H4 (Figure 2). The populations from the sampling sites of Kızkalesi, Mezitli, and Konacık were observed to contain more genetic variation, with three unique haplotypes in these regions. No correlation was identified between the genetic and morphological variations for the haplotypes. The highest divergence was in Konacık, where the main haplotype (H1) was separated by four mutation steps.

3.4. Species Delimitation Analysis

In total, five OTUs were assigned for all samples. *Botrylloides* cf. *lentus* (ON098245_1) was assigned in OTU-1, *Symplegma brakenhielmi* (LS992554_1) in OTU-2, all 27 *Botrylloides niger*/*nigrum*/*aff. leachii* reference samples together with all 11 from the present study in OTU-3, two uncharacterized *Botrylloides sp.* samples in OTU-4, and the 54 reference samples of *Botrylloides diegensis*/*leachii* in OTU-5 (Figure 3). All the main lineages reached 100% support, with some peripheral lineages having support as low as 60%. ASAP and PTP results supported identical species clustering (Figure S5).

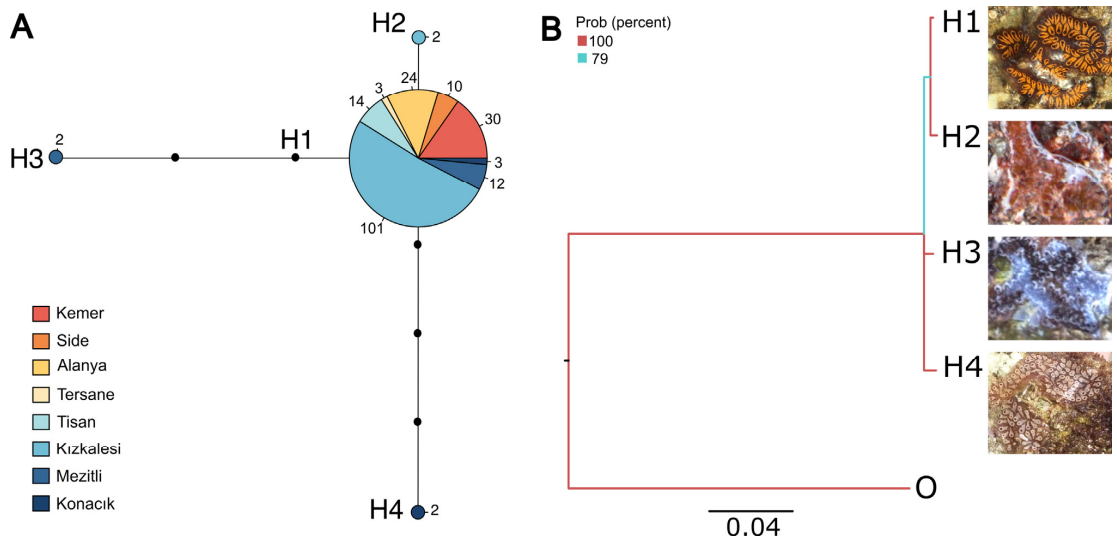

Figure 2. COI haplotype network of *B. niger* from the NEMS. (**A**) Minimum spanning network based on COI haplotypes of *B. niger* locus, overlaid with the corresponding haplotype name. Size differences of the circles indicate frequency, while colors reflect the regions where the colony was sampled. Numbers represent the number of samples in each category, and each correcting edge indicates a distance of one mutation step between the haplotypes. (**B**) Phylogenetic distance between the COI haplotypes is depicted by the best Bayesian tree, together with representative images of each haplotype. The branch colors represent bootstrap probability. The tree was rooted with the outgroup species *Symplegma brakenhielmi*.

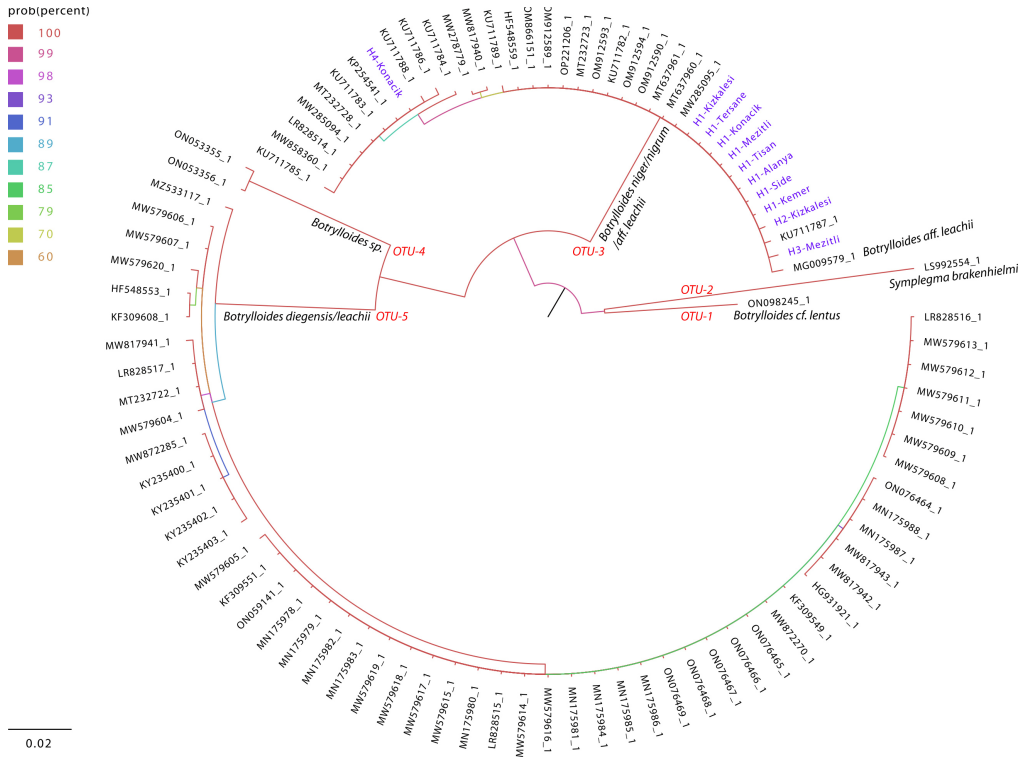

Figure 3. Bayesian majority rule consensus tree, reconstructed from the 519 bp COI sequence alignment. Support value is color-coded, as depicted on the left side of the tree. Corresponding OTUs, as determined by the ASAP and bPTP analyses, are written at the root of each group. The distance scale is given under the tree.

3.5. Species Assignment by DNA Barcoding Analysis

The final length of aligned and trimmed COI partial sequences was 519 bp. In total, we analyzed 203 COI sequences from the NEMS. The divergence among the studied populations was 0–0.4% (Table 1). The greatest distance was observed between the Konacık and the rest of the NEMS populations. The *B. aff. leachii* (MG009579) and *B. niger* (MW858360, LR828514, MW278779) database sequences diverged by less than 1% from the present populations. The distances between the NEMS samples and the database reference *B. leachii*/*B. diegensis* samples were ~17–23%.

Table 1. Pairwise mean COI distances between the NEMS populations and reference populations.

	1	2	3	4	5	6	7	8	9	10	11	12	13	14	15	16
1. Kızkalesi	-															
2. Mezitli	0.001	-														
3. Tershane	0.000	0.001	-													
4. Alanya	0.000	0.001	0.000	-												
5. Side	0.000	0.001	0.000	0.000	-											
6. Kemer	0.000	0.001	0.000	0.000	0.000	-										
7. Tisan	0.000	0.001	0.000	0.000	0.000	0.000	-									
8. Konacık	0.003	0.004	0.003	0.003	0.003	0.003	0.003	-								
9. BN-IL	0.000	0.001	0.000	0.000	0.000	0.000	0.000	0.003	-							
10. BL-IL	0.004	0.005	0.004	0.004	0.004	0.004	0.004	0.007	0.004	-						
11. BN-US	0.005	0.005	0.005	0.005	0.005	0.005	0.005	0.005	0.005	0.008	-					
12. BN-BR	0.008	0.008	0.008	0.008	0.008	0.008	0.008	0.005	0.008	0.011	0.005	-				
13. BL-IT	0.169	0.169	0.169	0.169	0.169	0.169	0.169	0.174	0.169	0.176	0.175	0.180	-			
14. BD-FR	0.196	0.195	0.196	0.196	0.196	0.196	0.196	0.201	0.196	0.192	0.202	0.209	0.008	-		
15. BL-ES	0.197	0.196	0.197	0.197	0.197	0.197	0.197	0.200	0.197	0.187	0.202	0.204	0.009	0.000	-	
16. BL-FR	0.230	0.230	0.230	0.230	0.230	0.230	0.230	0.232	0.230	0.234	0.232	0.234	0.196	0.203	0.199	-
17. Out-group	0.227	0.226	0.227	0.227	0.227	0.227	0.227	0.230	0.227	0.218	0.233	0.235	0.216	0.236	0.215	0.268

We sequenced 46 samples for the H3, three samples for the 18S, and two samples for the 28S genomic region. These sequences paired with at least 99% similarity to the reference sequences of *B. aff. leachii* (Figure S6) [10].

3.6. Spatial Diversity Analysis Based on COI

The evaluated regional population genetic diversity metrics (Table 2) showed that, despite its lower sample size (n = 5), the highest polymorphism (N_p = 4), haplotype diversity (N_h = 0.6), and nucleotide diversity (π = 0.0046) were measured in the Konacık population. No polymorphism was documented among the Tisan, Alanya, Side, Tersane, or Kemer populations.

Table 2. Genetic diversity indices and neutrality test statistics per NEMS geographical population based on COI sequences. Sequence numbers (n), number of polymorphic sites (N_p), number of haplotypes (N_h), observed haplotypes (H), nucleotide diversity (π), haplotype diversity (H_d), Fu and Li's D (F and LD), Fu and Li's F (F and LF), and Tajima's D (TajD). [a]: These groups have small population sizes (n < 10). Statistical significance: $p < 0.05$ (*).

Populations	n	N_p	N_h	H	π	H_d	F and LD	F and LF	TajD
Kemer	30	0	1	H1	0	0	0	0 [NS]	0
Side	10	0	1	H1	0	0	0	0 [NS]	0
Alanya	24	0	1	H1	0	0	0	0 [NS]	0
Tersane [a]	3	0	1	H1	0	0	0 [a]	0 [a]	0 [a]
Tisan	14	0	1	H1	0	0	0	0 [NS]	0
Kızkalesi	38	1	2	H1, H2	0.0001	0.053	−1.758	−1.823	−1.129
Mezitli	14	3	2	H1, H3	0.0015	0.264	1.070	0.757	−0.494
Konacık [a]	5	4	2	H1, H4	0.0046	0.600	1.641 [a]	1.670 [a]	1.641 [a]
All	138	7	4	H1, H2, H3, H4	0.0004	0.071	0.257	−0.557	−1.857 *

Fu and Li's D and Fu, Li's F, and Tajima's D tests were utilized to examine the neutrality of the mutations (Table 2). While no test was statistically significant at the level of geographical sub-populations, Tajima's D value for all the NEMS populations was significant negative (−1.857, $p < 0.05$).

Pairwise genetic differentiation (F_{st}) estimations (Table 3) showed that the Kemer-Mezitli pair was the only one that showed a statistically significant differentiation.

Table 3. Genetic differentiation (F_{st}) between the spatial populations. The statistical significance for F_{st} is indicated. [a]: These groups have small population sizes ($n < 10$). Statistical significance: p-value < 0.05 (*); n.c.: not calculated due to a lack of polymorphism.

F_{st}	Kemer	Side	Alanya	Tersane [a]	Tisan	Kızkalesi	Mezitli	Konacık [a]
Kemer	-	n.c.	n.c.	n.c.	n.c.	0	0.08 *	0.25 [a]
Side	-	-	n.c.	n.c.	n.c.	0	0.08	0.25 [a]
Alanya	-	-	-	n.c.	n.c.	0	0.08	0.25 [a]
Tersane [a]	-	-	-	-	n.c.	0 [a]	0.08 [a]	0.25 [a]
Tisan	-	-	-	-	-	0	0.08	0.25 [a]
Kızkalesi	-	-	-	-	-	-	0.07	0.25 [a]
Mezitli	-	-	-	-	-	-	-	0.17 [a]
Konacık [a]	-	-	-	-	-	-	-	-

Population size changes raggedness statistic (r) indicated that the only significant result was recorded for the Side population (Figure S7).

3.7. Temporal Diversity Analysis Based on COI

The genetic diversity metrics for the Kızkalesi time-series (Table 4) showed two haplotypes and one polymorphic site. The highest nucleotide and haplotype diversities were observed within the November population ($\pi = 0.0002$, $H_d = 0.111$), while no diversity was observed for the August–September period. The same polymorphism ($N_p = 1$) was recorded within the November and September populations.

Table 4. Genetic diversity indices and neutrality test statistics per Kızkalesi temporal population. Sequence numbers (n), number of polymorphic sites (N_p), number of haplotypes (N_h), nucleotide diversity (π), haplotype diversity (H_d), Fu and Li's D* (F and LD), Fu and Li's F* (F and LF) and Tajima's D (TajD). No value was measured with a statistically significant p-value < 0.05.

Populations	n	N_p	N_h	π	H_d	F and LD	F and LF	TajD
November 2017	18	1	2	0.0002	0.111	−1.450	−1.612	−1.165
July 2018	4	0	1	0	0	0	0	0
August 2018	17	0	1	0	0	0	0	0
September 2018	26	0	1	0	0	0	0	0
October 2018	38	1	2	0.0001	0.053	−1.758	−1.823	−1.129
All	103	1	2	0.0001	0.038	0.491	0.080	−0.912

The neutrality test statistics (Table 4) showed no statistically significant values for any population, but negative TajD values for the November and October populations. Pairwise genetic differentiation (F_{st}) and the population size changes raggedness statistic (r) showed no significant values for any of the temporal populations (Figure S8 and Table S8).

4. Discussion

In the present study, one primary (COI) and three additional molecular markers (H3, r18S, and r28S) were used to identify the genetic diversity of the *B. niger* colonies from the NEMS coasts of Türkiye. Taxonomical assignment based on the morphology of the samples was limited to the genus level (i.e., as a *Botrylloides* sp.) due to the high similarities between the sister species of this taxon [10,38,47,78]. Although the type of larval

incubation and the structure of the pyloric cecum have been reported to support species differentiation [38], these features are very challenging to precisely assess during punctual field sampling.

The morphological characteristics of the ascidians, as a tool to distinguish species and genera, have remained cryptic, without consensus. According to Van Name [79] and Boyd et al. [80], morphological variations are accepted to have no taxonomic importance for ascidians. On the other hand, Tarjuelo et al. [81] suggested that it is possible to differentiate the color morphs of *Pseudodistoma crucigaster*, a colonial ascidian, based on COI locus. Furthermore, a recent study proposes that although there are morphological overlaps between *Botryllus* and *Botrylloides*, they possess different features [78]. While this proposition keeps the two genera separated, the morphological separation within *Botrylloides* remains untangled. Aside from the general morphological confusion of *B. niger* with its sister species *B. leachii*, *B. diegensis*, or *B. violaceus*, the color morphs that were given for *Botrylloides simodensis* and *Botrylloides praelongus* significantly resemble some morphs of the NEMS colonies, highlighting that *Botrylloides* species share highly similar morphotypes [82].

Based on our morphological examination, a ladder-like "leachii type" zooid organization was found in all NEMS colonies [38]. At least 14 major morphotypes with various types of striped pigmentation were recorded as sub-morphs within the NEMS. The morphological diversity was similar to the description of Sheets et al. [6], who indicated 8 different morphotypes for *B. niger* for the 16 worldwide locations. We observed most of the indicated morphotypes in our NEMS colonies, with the addition of a frequent green-violet morph that was not documented in their study. In this study, we assumed that *B. niger* had been introduced to the Mediterranean basin from the Atlantic Ocean, from which it has been proposed to originate [6]. However, the greater number of morphotypes that we found in the NEMS is challenging this hypothesis, since greater diversity suggests fewer bottlenecked populations and, thus, potentially fewer migrations. Similarly, a significant morph variation of *B. schlosseri* was recorded for the Mediterranean colonies, which suggested that different pigmentation patterns might result in different adaptive fitness levels [51]. Moreover, Mediterranean colonies of *B. schlosseri* indicated a mixture of native and non-native sub-species with diverse origins from the Pacific to the Atlantic [83,84]. Thus, to understand the history of *B. niger*, broader sampling is needed.

The variation in the life history characteristics of colonial ascidians is shaped by their high phenotypic and genetic plasticity to environmental changes [37,85]. Monitoring the blastogenic cycles of the different morphs showed that for all colonies, the blastogenic stages (A–D) were sequential, with a duration that varied from 4 to 7 days. These results are congruent with the previously suggested cycle duration of about one week [23,30]. The shorter cycles are probably related to hibernation [51,86]. We observed that most of the hibernating colonies in the lab were unable to recover. Hyams et al. [86] stated that ~80% of the hibernating colonies died within five months of the hibernation period. Hibernation seems to be one of the main reasons for the short life span of the colonies. To understand hibernation in their natural environment, we recorded the colonial diversity of our samplings in the winter period. We did not observe any colonies during the winter in the intertidal zone, where we collected our samples regularly.

The measured negative TajD value supports this interpretation of population expansion after a selective sweep, albeit without being statistically significant. However, Fu and Li's D* and Fu and Li's F* non-significant values suggest the opposite process, implying that the population has not undergone recent demographic or selective events. This apparent contradiction might be due to our sampling strategy. Indeed, F and LD and F and LF have notably little detection power for growing populations if the sampling rate is not focused around the period of maximal growth rate [87]. Consequently, having one single sampling period during August might prevent these two tests from detecting the selective sweep measured by TajD. Monitoring the colonies over more than one year, or at a higher frequency during summer, would help to clarify the demographic and selective processes that may affect the population.

Along with the morphological and life history characterization of the NEMS population, we also conducted genetic analyses. Molecular comparisons with the GenBank data showed that the current study sequences match 99–100 % with the *B. niger* sequences based on the COI locus; thus, we classified our species as *Botrylloides niger*. We found five OTUs based on our species delimitation analyses. OTU-3 consisted of all the *B. niger* haplotypes of the current study together with the GenBank *B. niger/nigrum/aff. leachii* sequences. The out-group (*Symplegma brakenhielmi*) and the other *Botrylloides* species, such as *Botrylloides diegensis*, were located in separate taxonomic units. We thus support COI as an adequate marker to identify and separate *Botrylloides* species, and *B. niger* in particular. Furthermore, our H3, r18S, and r28S sequences congruently matched with the same Israeli *B. aff. leachii* sequences whose COI barcode matched our COI barcode 100 % [10].

Despite covering only 8 stations along an 800 km coastline, the studied NEMS colonies demonstrated significant diversity, encompassing 14 morphotypes, 4 COI haplotypes, and 14 H3 genotypes. Furthermore, the overall haplotype diversity of COI was low (π_{COI}: 0.0004), which might stem from a recent bottleneck of the mitochondrial genome or from high introgression rates. Similarly, Sheets et al. [6] found low diversity of the *B. niger* populations on the Atlantic and Pacific coasts of COI and ANT loci.

Considering the significant negative Tajima's D values, the null hypothesis that the colonies of Türkiye's NEMS were overall under negative selection for COI was not rejected. The NEMS population seems to be under purifying selection, expanding from a restricted population or a selective sweep.

Likewise, Sheets et al. [6] found the *B. niger* populations on the Atlantic coast of Panama, the Pacific coast of Panama, and the coasts of Mexico to be under negative selection for the COI locus, which suggests a small population size, a founder effect, or a low dispersal. The selective forces acting as the environmental stressors on the mitochondrial DNA might be salinity or temperature [88–90].

The demographic population analyses based on the COI gene showed that the Side population was under significant subdivision, which could very likely result from major local freshwater input (the Manavgat stream). Freshwater inputs are known to cause the coastal salinity values to fluctuate. In support of this, Karahan et al. [91] stated that the dynamics of *B. schlosseri* populations from the California coasts were dramatically affected upon flooding events. Moreover, *B. violaceus* larvae exposed to low salinity were shown to express osmotic stress with an increased mortality rate, suggesting that colonial fitness would be reduced by seasonal storm events that cause seawater salinity to fluctuate [92]. Since the lowest salinity record (37.5 ppt) among the sampling stations belonged to Side, the population structure of the *B. niger* colonies appears to be affected by the lower salinity.

In this study, the population structures and interactions of *B. niger* from the NEMS were investigated using four molecular markers for eight spatial stations and one time-series station. Morphological results showed similar colonial characteristics regarding the blastogenic cycle and hibernation, but with a greater number of new morphotype records. Concerning the ambiguities in the classification of *Botrylloides*, previously suggested molecular markers were used to identify the populations from the Turkish coasts of the NEMS. As a result, the COI marker was observed to provide sufficient identification of the species.

Supplementary Materials: The following supporting information can be downloaded at: https://www.mdpi.com/article/10.3390/d15030367/s1. Figure S1: Description of the 14 morphotypes. Figure S2: Morphology of *Botrylloides niger*. Figure S3: The blastogenic cycle of *B. niger*. Figure S4: Hibernation of *B. niger*. Figure S5: Delimiting Operational Taxonomic Units (OTUs) and Bayesian tracer. Figure S6: Nuclear gene analyses of *B. niger*. Figure S7: Population size changes analysis based on the mismatch distribution of the COI gene for Kızkalesi, Mezitli, Konacık, and all populations. Figure S8: Population size changes of Kızkalesi time-series station based on mismatch distribution of COI. Table S1: Details of sampling stations. Table S2: Details of samplings and observed haplotypes and genotypes. Table S3: Kızkalesi site time-series samplings. Table S4: PCR programs for COI, H3, 28S rRNA and 18S rRNA genes. Table S5: Primers used in the present study. Table S6: Accession numbers for the GenBank reference sequences. Table S7: Life history of the 19 colonies cultured in the laboratory. Table S8:

Pairwise comparison of the genetic differentiation (Fst) between the temporal populations of Kızkalesi. Table S9: Correspondence between sample IDs, morphotypes and the determined haplotypes and genotypes for COI, H3, 18S and 28S.

Author Contributions: Conceptualization, B.T. and A.K.; data curation, B.T., E.Ö. and A.K.; methodology, B.T., E.Ö., S.B. and A.K.; writing—original draft, B.T., S.B. and A.K. All authors have read and agreed to the published version of the manuscript.

Funding: This study was supported by the YÖP-701-2018-2666 project (Middle East Technical University support program) and BAP-08-11-DPT2012K120880 for B.T., E.Ö and A.K.; and by the Swiss National Science Foundation (SNF) [grant number PZ00P3_173981] for S.B.

Institutional Review Board Statement: The study was conducted in accordance with the Animal testing regulations Directive 2010/63/EU and the national regulation of Türkiye.

Data Availability Statement: Sequences, trace files, image files, and the primer information for each of the four COI haplotype were uploaded to the Barcode of Life Data System [5] with the accession numbers IMS255-19, IMS256-19, FEE003-23, and FEE007-23, all grouped under the BOLD:ACI1328 BIN code. COI haplotype sequences were also uploaded to NCBI GenBank [4] with accession numbers OQ211497, OQ211498, OQ211500 and OQ211501. Similarly, the 14 Histone 3, the three 18S rRNA, and the two 28S rRNA sequences were submitted to BOLD with accession numbers FEE003-23, FEE007-23, FEE012-23 to FEE025-23 and IMS254-19 to IMS257-19, as well as to GenBank; accession numbers are pending attribution. Accession numbers of the COI sequences taken from GenBank are provided in Table S6 (data retrieved from the NCBI in September 2022). Haplotypes of the sampled colonies are provided in Table S9.

Acknowledgments: We thank Megan Wilson and Michael Hart for their valuable comments on the final version of the manuscript. We thank Baruch Rinkevich, Jacob Douek, and Guy Paz for their endless support and Kenan Murat Karahan for sampling help. We kindly thank Oscar Dalkjaer Wigant, Sonja Hummel and Aude Blanchoud for proofreading the manuscript. We thank Side and Erdemli Municipality for their kind assistance during our samplings. We also thank the anonymous reviewers for their helpful comments.

Conflicts of Interest: The authors declare no conflict of interest.

References

1. Avise, J.C. Phylogeography: Retrospect and Prospect. *J. Biogeogr.* **2009**, *36*, 3–15. [CrossRef]
2. Bowen, B.W.; Gaither, M.R.; DiBattista, J.D.; Iacchei, M.; Andrews, K.R.; Grant, W.S.; Toonen, R.J.; Briggs, J.C. Comparative Phylogeography of the Ocean Planet. *Proc. Natl. Acad. Sci. USA* **2016**, *113*, 7962–7969. [CrossRef] [PubMed]
3. Seebens, H.; Schwartz, N.; Schupp, P.J.; Blasius, B. Predicting the Spread of Marine Species Introduced by Global Shipping. *Proc. Natl. Acad. Sci. USA* **2016**, *113*, 5646–5651. [CrossRef]
4. Benson, D.A.; Karsch-Mizrachi, I.; Clark, K.; Lipman, D.J.; Ostell, J.; Sayers, E.W. GenBank. *Nucleic Acids Res.* **2012**, *40*, D48–D53. [CrossRef]
5. Ratnasingham, S.; Hebert, P.D.N. Bold: The Barcode of Life Data System (http://www.barcodinglife.org). *Mol. Ecol. Notes* **2007**, *7*, 355–364. [CrossRef] [PubMed]
6. Sheets, E.A.; Cohen, C.S.; Ruiz, G.M.; da Rocha, R.M. Investigating the Widespread Introduction of a Tropical Marine Fouling Species. *Ecol. Evol.* **2016**, *6*, 2453–2471. [CrossRef]
7. Villalobos, S.M.; Lambert, G.; Shenkar, N.; López-Legentil, S. Distribution and Population Dynamics of Key Ascidians in North Carolina Harbors and Marinas. *Aquat. Invasions* **2017**, *12*, 447–458. [CrossRef]
8. Reem, E.; Douek, J.; Rinkevich, B. A Critical Deliberation of the 'Species Complex' Status of the Globally Spread Colonial Ascidian *Botryllus schlosseri*. *J. Mar. Biol. Assoc. UK* **2021**, *101*, 1047–1060. [CrossRef]
9. Karahan, A.; Douek, J.; Paz, G.; Stern, N.; Kideys, A.E.; Shaish, L.; Goren, M.; Rinkevich, B. Employing DNA Barcoding as Taxonomy and Conservation Tools for Fish Species Censuses at the Southeastern Mediterranean, a Hot-Spot Area for Biological Invasion. *J. Nat. Conserv.* **2017**, *36*, 1–9. [CrossRef]
10. Reem, E.; Douek, J.; Rinkevich, B. Ambiguities in the Taxonomic Assignment and Species Delineation of Botryllid Ascidians from the Israeli Mediterranean and Other Coastlines. *Mitochondrial DNA A DNA Mapp. Seq. Anal.* **2018**, *29*, 1073–1080. [CrossRef]
11. Eryilmaz, L.; Dalyan, C. First Record of *Apogon queketti* Gilchrist (Osteichthyes: Apogonidae) in the Mediterranean Sea. *J. Fish Biol.* **2006**, *69*, 1251–1254. [CrossRef]
12. Smith, M.A.; Poyarkov, N.A.; Hebert, P.D.N. CO1 DNA Barcoding Amphibians: Take the Chance, Meet the Challenge. *Mol. Ecol. Resour.* **2008**, *8*, 235–246. [CrossRef]

13. Keskin, E.; Atar, H.H. DNA Barcoding Commercially Important Fish Species of Turkey. *Mol. Ecol. Resour.* **2013**, *13*, 788–797. [CrossRef]
14. Oter, K.; Gunay, F.; Tuzer, E.; Linton, Y.M.; Bellini, R.; Alten, B. First Record of *Stegomyia albopicta* in Turkey Determined By Active Ovitrap Surveillance and DNA Barcoding. *Vector-Borne Zoonotic Dis.* **2013**, *13*, 753–761. [CrossRef] [PubMed]
15. Azzurro, E.; Goren, M.; Diamant, A.; Galil, B.; Bernardi, G. Establishing the Identity and Assessing the Dynamics of Invasion in the Mediterranean Sea by the Dusky Sweeper, *Pempheris rhomboidea* Kossmann & Rauber, 1877 (Pempheridae, Perciformes). *Biol. Invasions* **2015**, *17*, 815–826. [CrossRef]
16. Bariche, M.; Torres, M.; Smith, C.; Sayar, N.; Azzurro, E.; Baker, R.; Bernardi, G. Red Sea Fishes in the Mediterranean Sea: A Preliminary Investigation of a Biological Invasion Using DNA Barcoding. *J. Biogeogr.* **2015**, *42*, 2363–2373. [CrossRef]
17. Seyhan, D.; Turan, C. DNA Barcoding of Scombrid Species in the Turkish Marine Waters. *J. Black Sea-Mediterr. Environ.* **2016**, *22*, 35–45.
18. Tuney, I. Molecular Identification of Puffer Fish *Lagocephalus sceleratus* (Gmelin, 1789) and *Lagocephalus spadiceus* (Richardson, 1845) from Eastern Mediterranean, Turkey. *Fresenius Environ. Bull.* **2016**, *25*, 1429–1437.
19. Ciftci, O.; Karahan, A.; Orek, Y.A.K.; Kideys, A.E. First Record of the Buccaneer Anchovy *Encrasicholina punctifer* (Fowler, 1938) (Clupeiformes; Engraulidae) in the Mediterranean Sea, Confirmed through DNA Barcoding. *J. Appl. Ichthyol.* **2017**, *33*, 520–523. [CrossRef]
20. Ozbek, E.O.; Mavruk, S.; Saygu, I.; Ozturk, B. Lionfish Distribution in the Eastern Mediterranean Coast of Turkey. *J. Black Sea-Mediterr. Environ.* **2017**, *23*, 1–16.
21. Golestani, H.; Crocetta, F.; Padula, V.; Camacho-Garcia, Y.; Langeneck, J.; Poursanidis, D.; Pola, M.; Yokes, M.B.; Cervera, J.L.; Jung, D.W.; et al. The Little *Aplysia* Coming of Age: From One Species to a Complex of Species Complexes in *Aplysia parvula* (Mollusca: Gastropoda: Heterobranchia). *Zool. J. Linn. Soc.* **2019**, *187*, 279–330. [CrossRef]
22. Shenkar, N.; Swalla, B.J. Global Diversity of Ascidiacea. *PLoS ONE* **2011**, *6*, e20657. [CrossRef]
23. Berrill, N.J. The Developmental Cycle of *Botrylloides*. *Q. J. Microsc. Sci.* **1947**, *88*, 393–407. [CrossRef] [PubMed]
24. Sabbadin, A. Experimental Analysis of the Development of Colonies of *Botryllus schlosseri* (Pallas) [Ascidiacea]. *Arch. Ital. Anat. Embriol.* **1958**, *63*, 178–221.
25. Manni, L.; Anselmi, C.; Cima, F.; Gasparini, F.; Voskoboynik, A.; Martini, M.; Peronato, A.; Burighel, P.; Zaniolo, G.; Ballarin, L. Sixty Years of Experimental Studies on the Blastogenesis of the Colonial Tunicate *Botryllus schlosseri*. *Dev. Biol.* **2019**, *448*, 293–308. [CrossRef] [PubMed]
26. Paz, G.; Rinkevich, B. Morphological Consequences for Multi-Partner Chimerism in *Botrylloides*, a Colonial Urochordate. *Dev. Comp. Immunol.* **2002**, *26*, 615–622. [CrossRef] [PubMed]
27. Rinkevich, B. Natural Chimerism in Colonial Urochordates. *J. Exp. Mar. Biol. Ecol.* **2005**, *322*, 93–109. [CrossRef]
28. Zondag, L.E.; Rutherford, K.; Gemmell, N.J.; Wilson, M.J. Uncovering the Pathways Underlying Whole Body Regeneration in a Chordate Model, *Botrylloides leachi* Using de Novo Transcriptome Analysis. *BMC Genom.* **2016**, *17*, 114. [CrossRef]
29. Blanchoud, S.; Zondag, L.; Lamare, M.D.; Wilson, M.J. Hematological Analysis of the Ascidian *Botrylloides leachii* (Savigny, 1816) during Whole-Body Regeneration. *Biol. Bull.* **2017**, *232*, 143–157. [CrossRef]
30. Blanchoud, S.; Rinkevich, B.; Wilson, M.J. Whole-Body Regeneration in the Colonial Tunicate *Botrylloides leachii*. *Results Probl. Cell Differ.* **2018**, *65*, 337–355. [CrossRef]
31. Karahan, A.; Öztürk, E.; Temiz, B.; Blanchoud, S. Studying Tunicata WBR Using *Botrylloides anceps*. In *Whole-Body Regeneration*; Springer Humana: New York, NY, USA, 2022; pp. 311–332.
32. Viard, F.; Roby, C.; Turon, X.; Bouchemousse, S.; Bishop, J. Cryptic Diversity and Database Errors Challenge Non-Indigenous Species Surveys: An Illustration With *Botrylloides* spp. in the English Channel and Mediterranean Sea. *Front. Mar. Sci.* **2019**, *6*, 615. [CrossRef]
33. Spallanzani, L. Storia naturale del mare. 1784. Unpublished. Available online: https://sites.google.com/site/ascidianbiologylab/clients (accessed on 28 February 2023).
34. Olivi, G. Zoologica Adriatica. *Biodivers. Herit. Libr.* 1792. Available online: https://www.marinespecies.org/aphia.php?p=taxdetails&id=542267 (accessed on 28 February 2023).
35. Savigny, J.C. *Memoires Sur Les Animaux sans Vertebres*; Deterville: Paris, France, 1816. [CrossRef]
36. Pinar, E. Fouling and Boring Organisms in Some Turkish Harbours and the Effectivity of Antifouling and Antiboring Paint against These Organisms. *Sci. Rep. Fac. Sci. Ege Univ.* **1974**, *170*, 1–67. (In Turkish)
37. Rinkevich, B.; Shlemberg, Z.; Lilker-Levav, T.; Goren, M.; Fishelson, L. Life History Characteristics of *Botrylloides* (Tunicata) Populations in Akko Bay, Mediterranean Coast of Israel. *Isr. J. Ecol. Evol.* **1993**, *39*, 197–212. [CrossRef]
38. Brunetti, R. Botryllid Species (Tunicata, Ascidiacea) from the Mediterranean Coast of Israel, with Some Considerations on the Systematics of *Botryllinae*. *Zootaxa* **2009**, *2289*, 18–32. [CrossRef]
39. Brunetti, R.; Mastrototaro, F. *Botrylloides Pizoni*, a New Species of *Botryllinae* (Ascidiacea) from the Mediterranean Sea. *Zootaxa* **2012**, *3258*, 28–36. [CrossRef]
40. Cinar, M.E. Checklist of the Phyla Platyhelminthes, Xenacoelomorpha, Nematoda, Acanthocephala, Myxozoa, Tardigrada, Cephalorhyncha, Nemertea, Echiura, Brachiopoda, Phoronida, Chaetognatha, and Chordata (Tunicata, Cephalochordata, and Hemichordata) from the Coasts of Turkey. *Turk. J. Zool.* **2014**, *38*, 698–722.

41. Halim, Y.; Messeih, M.A. Aliens in Egyptian Waters. A Checklist of Ascidians of the Suez Canal and the Adjacent Mediterranean Waters. *Egypt. J. Aquat. Res.* **2016**, *42*, 449–457. [CrossRef]
42. Herdman, W.A. Report on the Tunicata Collected during the Years 1873-1876. Part 2, Ascidiae Compositae. *Zool. Chall. Exp.* **1886**, *14*, 1–425.
43. Sluiter, C.P. Tuniciers Recueilli En 1896, Par La Chazalie, Dans La Mer Des Antilles. *Mém. Société Zool. Fr.* **1898**, *11*, 5–34.
44. Pérès, J.M. Ascidies Recoltées Sur Les Cotes Mediterraneenaires d'Israel. *Bull. Res. Counc. Isr.* **1958**, *7B*, 143–150.
45. Griggio, F.; Voskoboynik, A.; Iannelli, F.; Justy, F.; Tilak, M.-K.; Xavier, T.; Pesole, G.; Douzery, E.J.P.; Mastrototaro, F.; Gissi, C. Ascidian Mitogenomics: Comparison of Evolutionary Rates in Closely Related Taxa Provides Evidence of Ongoing Speciation Events. *Genome Biol. Evol.* **2014**, *6*, 591–605. [CrossRef]
46. Rubinstein, N.D.; Feldstein, T.; Shenkar, N.; Botero-Castro, F.; Griggio, F.; Mastrototaro, F.; Delsuc, F.; Douzery, E.J.; Gissi, C.; Huchon, D. Deep Sequencing of Mixed Total DNA without Barcodes Allows Efficient Assembly of Highly Plastic Ascidian Mitochondrial Genomes. *Genome Biol. Evol.* **2013**, *5*, 1185–1199. [CrossRef] [PubMed]
47. Salonna, M.; Gasparini, F.; Huchon, D.; Montesanto, F.; Haddas-Sasson, M.; Ekins, M.; McNamara, M.; Mastrototaro, F.; Gissi, C. An Elongated COI Fragment to Discriminate Botryllid Species and as an Improved Ascidian DNA Barcode. *Sci. Rep.* **2021**, *11*, 4078. [CrossRef] [PubMed]
48. Virgili, R.; Tanduo, V.; Katsanevakis, S.; Terlizzi, F.; Villani, G.; Fontana, A.; Crocetta, F. The Miseno Lake (Central-Western Mediterranean Sea): An Overlooked Reservoir of Non-Indigenous and Cryptogenic Ascidians in a Marine Reserve. *Front. Mar. Sci.* **2022**, *9*. [CrossRef]
49. Della Sala, G.; Coppola, D.; Virgili, R.; Vitale, G.A.; Tanduo, V.; Teta, R.; Crocetta, F.; de Pascale, D. Untargeted Metabolomics Yields Insights into the Lipidome of *Botrylloides Niger* Herdman, 1886, An Ascidian Invading the Mediterranean Sea. *Front. Mar. Sci.* **2022**, *9*, 866906. [CrossRef]
50. Micaroni, V.; Strano, F.; Crocetta, F.; Di Franco, D.; Piraino, S.; Gravili, C.; Rindi, F.; Bertolino, M.; Costa, G.; Langeneck, J.; et al. Project "Biodiversity MARE Tricase": A Species Inventory of the Coastal Area of Southeastern Salento (Ionian Sea, Italy). *Diversity* **2022**, *14*, 904. [CrossRef]
51. Cima, F.; Ballarin, L.; Caicci, F.; Franchi, N.; Gasparini, F.; Rigon, F.; Schiavon, F.; Manni, L. Life History and Ecological Genetics of the Colonial Ascidian *Botryllus schlosseri*. *Zool. Anz. -J. Comp. Zool.* **2015**, *257*, 54–70. [CrossRef]
52. Faber, K.L.; Person, E.C.; Hudlow, W.R. PCR Inhibitor Removal Using the NucleoSpin (R) DNA Clean-Up XS Kit. *Forensic Sci. Int.-Genet.* **2013**, *7*, 209–213. [CrossRef] [PubMed]
53. Larkin, M.A.; Blackshields, G.; Brown, N.P.; Chenna, R.; McGettigan, P.A.; McWilliam, H.; Valentin, F.; Wallace, I.M.; Wilm, A.; Lopez, R. Clustal W and Clustal X Version 2.0. *Bioinformatics* **2007**, *23*, 2947–2948. [CrossRef] [PubMed]
54. Hall, T.A. BioEdit: Version 7.0.0, A User-Friendly Biological Sequence Alignment Editor and Analysis Program for Windows 95/98/NT. *Nucleic Acids Symposium Series* **1999**, *41*, 95–98.
55. Excoffier, L.; Lischer, H.E. Arlequin Suite Ver 3.5: A New Series of Programs to Perform Population Genetics Analyses under Linux and Windows. *Mol. Ecol. Resour.* **2010**, *10*, 564–567. [CrossRef] [PubMed]
56. Teacher, A.G.F.; Griffiths, D.J. HapStar: Automated Haplotype Network Layout and Visualization. *Mol. Ecol. Resour.* **2011**, *11*, 151–153. [CrossRef] [PubMed]
57. Ronquist, F.; Teslenko, M.; Van Der Mark, P.; Ayres, D.L.; Darling, A.; Höhna, S.; Larget, B.; Liu, L.; Suchard, M.A.; Huelsenbeck, J.P. MrBayes 3.2: Efficient Bayesian Phylogenetic Inference and Model Choice across a Large Model Space. *Syst. Biol.* **2012**, *61*, 539–542. [CrossRef]
58. Lefort, V.; Longueville, J.-E.; Gascuel, O. SMS: Smart Model Selection in PhyML. *Mol. Biol. Evol.* **2017**, *34*, 2422–2424. [CrossRef] [PubMed]
59. Rambaut, A. FigTree v1.4.4. Available online: http://tree.bio.ed.ac.uk/software/figtree/ (accessed on 24 November 2022).
60. Puillandre, N.; Brouillet, S.; Achaz, G. ASAP: Assemble Species by Automatic Partitioning. *Mol. Ecol. Resour.* **2021**, *21*, 609–620. [CrossRef] [PubMed]
61. Zhang, J.; Kapli, P.; Pavlidis, P.; Stamatakis, A. A General Species Delimitation Method with Applications to Phylogenetic Placements. *Bioinformatics* **2013**, *29*, 2869–2876. [CrossRef] [PubMed]
62. Jukes, T.H.; Cantor, C.R. Evolution of Protein Molecules. *Mamm. Protein Metab.* **1969**, *3*, 21–132.
63. Kimura, M. A Simple Method for Estimating Evolutionary Rates of Base Substitutions through Comparative Studies of Nucleotide Sequences. *J. Mol. Evol.* **1980**, *16*, 111–120. [CrossRef] [PubMed]
64. Nei, M.; Kumar, S. *Molecular Evolution and Phylogenetics*; Oxford University Press: Oxford, UK, 2000.
65. Kumar, S.; Stecher, G.; Li, M.; Knyaz, C.; Tamura, K. MEGA X: Molecular Evolutionary Genetics Analysis across Computing Platforms. *Mol. Biol. Evol.* **2018**, *35*, 1547–1549. [CrossRef]
66. Johnson, M.; Zaretskaya, I.; Raytselis, Y.; Merezhuk, Y.; McGinnis, S.; Madden, T.L. NCBI BLAST: A Better Web Interface. *Nucleic Acids Res.* **2008**, *36*, W5–W9. [CrossRef]
67. Rozas, J.; Ferrer-Mata, A.; Sanchez-DelBarrio, J.C.; Guirao-Rico, S.; Librado, P.; Ramos-Onsins, S.E.; Sanchez-Gracia, A. DnaSP 6: DNA Sequence Polymorphism Analysis of Large Data Sets. *Mol. Biol. Evol.* **2017**, *34*, 3299–3302. [CrossRef] [PubMed]
68. Nei, M.; Li, W.-H. Mathematical Model for Studying Genetic Variation in Terms of Restriction Endonucleases. *Proc. Natl. Acad. Sci. USA* **1979**, *76*, 5269–5273. [CrossRef]
69. Nei, M. *Molecular Evolutionary Genetics*; Columbia University Press: New York, NY, USA, 1987.

70. Fu, Y.-X.; Li, W.-H. Statistical Tests of Neutrality of Mutations. *Genetics* **1993**, *133*, 693–709. [CrossRef]
71. Tajima, F. Evolutionary Relationship of DNA Sequences in Finite Populations. *Genetics* **1983**, *105*, 437–460. [CrossRef] [PubMed]
72. Weir, B.S.; Cockerham, C.C. Estimating F-Statistics for the Analysis of Population Structure. *Evolution* **1984**, *38*, 1358–1370. [CrossRef] [PubMed]
73. Hudson, R.R.; Boos, D.D.; Kaplan, N.L. A Statistical Test for Detecting Geographic Subdivision. *Mol. Biol. Evol.* **1992**, *9*, 138–151.
74. Watterson, G.A. On the Number of Segregating Sites in Genetical Models without Recombination. *Theor. Popul. Biol.* **1975**, *7*, 256–276. [CrossRef]
75. Harpending, H.C. Signature of Ancient Population Growth in a Low-Resolution Mitochondrial DNA Mismatch Distribution. *Hum. Biol.* **1994**, *66*, 591–600.
76. Bah, T. *Inkscape: Guide to a Vector Drawing Program (Digital Short Cut)*; Pearson Education: London, UK, 2009; ISBN 0-13-705171-9.
77. Watanabe, H. Studies on the Regulation in Fused Colonies in *Botryllus primigenus* (Ascidiae Compositae). *Sci. Rep. Tokyo Bunrika Daigaku* **1953**, *7*, 183–198.
78. Nydam, M.L.; Lemmon, A.R.; Cherry, J.R.; Kortyna, M.L.; Clancy, D.L.; Hernandez, C.; Cohen, C.S. Phylogenomic and Morphological Relationships among the Botryllid Ascidians (*Subphylum tunicata*, *Class ascidiacea*, Family Styelidae). *Sci. Rep.* **2021**, *11*, 8351. [CrossRef]
79. Van Name, W.G. The North and South American Ascidians. *Bull. Am. Mus. Nat. Hist.* **1945**, *84*, 1–462.
80. Boyd, H.C.; Weissman, I.L.; Saito, Y. Morphologic and Genetic Verification That Monterey *Botryllus* and Woods Hole *Botryllus* Are the Same Species. *Biol. Bull.* **1990**, *178*, 239–250. [CrossRef] [PubMed]
81. Tarjuelo, I.; Posada, D.; Crandall, K.A.; Pascual, M.; Turon, X. Phylogeography and Speciation of Colour Morphs in the Colonial Ascidian *Pseudodistoma crucigaster*. *Mol. Ecol.* **2004**, *13*, 3125–3136. [CrossRef] [PubMed]
82. Atsumi, M.O.; Saito, Y. Studies on Japanese Botryllid Ascidians. V. A New Species of the Genus *Botrylloides* Very Similar to *Botrylloides Simodensis* in Morphology. *Zool. Sci.* **2011**, *28*, 532–542. [CrossRef]
83. Nydam, M.L.; Giesbrecht, K.B.; Stephenson, E.E. Origin and Dispersal History of Two Colonial Ascidian Clades in the *Botryllus schlosseri* Species Complex. *PLoS ONE* **2017**, *12*, e0169944. [CrossRef]
84. Ulman, A.; Ferrario, J.; Occhpinti-Ambrogi, A.; Arvanitidis, C.; Bandi, A.; Bertolino, M.; Bogi, C.; Chatzigeorgiou, G.; Çiçek, B.A.; Deidun, A. A Massive Update of Non-Indigenous Species Records in Mediterranean Marinas. *PeerJ* **2017**, *5*, e3954. [CrossRef]
85. Blanchoud, S.; Rutherford, K.; Zondag, L.; Gemmell, N.J.; Wilson, M.J. De Novo Draft Assembly of the *Botrylloides leachii* Genome Provides Further Insight into Tunicate Evolution. *Sci. Rep.* **2018**, *8*, 5518. [CrossRef]
86. Hyams, Y.; Paz, G.; Rabinowitz, C.; Rinkevich, B. Insights into the Unique Torpor of *Botrylloides leachi*, a Colonial Urochordate. *Dev. Biol.* **2017**, *428*, 101–117. [CrossRef]
87. Fu, Y.-X. Statistical Tests of Neutrality of Mutations Against Population Growth, Hitchhiking and Background Selection. *Genetics* **1997**, *147*, 915–925. [CrossRef]
88. Galtier, N.; Nabholz, B.; Glémin, S.; Hurst, G.D.D. Mitochondrial DNA as a Marker of Molecular Diversity: A Reappraisal. *Mol. Ecol.* **2009**, *18*, 4541–4550. [CrossRef]
89. Morin, P.A.; Foote, A.D.; Baker, C.S.; Hancock-Hanser, B.L.; Kaschner, K.; Mate, B.R.; Mesnick, S.L.; Pease, V.L.; Rosel, P.E.; Alexander, A. Demography or Selection on Linked Cultural Traits or Genes? Investigating the Driver of Low MtDNA Diversity in the Sperm Whale Using Complementary Mitochondrial and Nuclear Genome Analyses. *Mol. Ecol.* **2018**, *27*, 2604–2619. [CrossRef]
90. Wei, W.; Tuna, S.; Keogh, M.J.; Smith, K.R.; Aitman, T.J.; Beales, P.L.; Bennett, D.L.; Gale, D.P.; Bitner-Glindzicz, M.A.K.; Black, G.C.; et al. Germline Selection Shapes Human Mitochondrial DNA Diversity. *Science* **2019**, *364*, 6520. [CrossRef] [PubMed]
91. Karahan, A.; Douek, J.; Paz, G.; Rinkevich, B. Population Genetics Features for Persistent, but Transient, *Botryllus schlosseri* (Urochordata) Congregations in a Central Californian Marina. *Mol. Phylogenet. Evol.* **2016**, *101*, 19–31. [CrossRef] [PubMed]
92. Lambert, W.J.; Dijkstra, J.A.; Clark, E.; Connolly, J. Larval Exposure to Low Salinity Compromises Metamorphosis and Growth in the Colonial Ascidian *Botrylloides violaceus*. *Invertebr. Biol.* **2018**, *137*, 281–288. [CrossRef]